Measurement 176 (2021) 109211

Contents lists available at ScienceDirect

Measurement

journal homepage: www.elsevier.com/locate/measurement

Volumetric Motion Magnification: Subtle Motion Extraction from 4D Data

Matthew Southwick, Zhu Mao *, Christopher Niezrecki

Department of Mechanical Engineering, University of Massachusetts Lowell, Lowell, MA, USA

ARTICLE INFO

Keywords:
Phase-based motion magnification
Digital volume correlation
3D analysis
Modal analysis
Image processing

ABSTRACT

The extension of Phase-based Video Motion Magnification into three-dimensions is presented in this work. The technique uses a 3D complex steerable pyramid to decompose volumetric frames of 4D dataset. The resulting decomposition can be processed to filter, amplify, or attenuate subtle motions occurring locally within the 4D data, before inversion of the transform is performed to recreate the volumetric images. Recent research has used Phase Based Video Motion Magnification to extract subtle motion from 2D slices of internal deformation data. This work demonstrates how Phase Based Video Motion Magnification can be extended to work on full volumetric images to extract full 3D volumetric motions. The Volumetric Motion Magnification technique is demonstrated qualitatively, to amplify and extract the indiscernible motion of a cylinder for visual identification. Then, the ability of the technique to enhance the motion noise floor of Digital Volume Correlation by more than a factor of 10 is demonstrated.

1. Introduction

The study of structural deformation has been advanced in the past decade by the adaptation of optical motion measurement techniques to perform noncontact and full-field motion measurements. A major limitation of camera-based structural displacement measurement techniques is the necessity to maintain line of sight between cameras and the points of interest. For this reason, it is difficult or impossible to perform motion measurements of components internal to a structure. The majority of the dynamics in complicated structures occur out of line of sight, and often in locations inaccessible to traditional instrumentation. Because of this limitation, an increasing area of research involves using non-optical electromagnetic imaging to capture internal structural characteristics over the full volume, which changes over time. In this way, noncontact motion measurements of otherwise inaccessible structures are obtainable.

Complicated machines often have large numbers of tightly packaged components with unique structural behavior. For example, circuit boards buried in the heart of an assembly often fail due to vibration that is difficult to study experimentally in situ. These problems demand a volumetric imaging and motion analysis approach. This paper represents an additional tool for the analysis of subtle internal dynamics through volumetric imaging.

Volumetric Motion Magnification (VMM) is an extension of Phase-Based Video Motion Magnification (PBVMM) for use on full volumes sampled over time [1]. PBVMM is a technique using a complex steerable pyramid to extract spatially local motion at various spatial frequencies in the form of filter phase responses, within a video. The extracted filter phases are then filtered and amplified to create a new video with altered motion. PBVMM has been shown to have excellent noise handling characteristics and an outstanding ability to extract extremely subtle motion from video [2–5].

A large number of improvements and extensions to PBVMM have been made since its development in 2013. The focus of these developments has been in a number of areas. First, extensive work has gone into the amplification of subtle motion in the presence of large motions [6–8] for system dynamics identification. Second, computational efficiency of PBVMM has been explored through use of sophisticated filtering techniques [9–10]. And third, the ability to accurately reconstruct the video with the true subtle motion has been handled by work on improving artifact generation and noise handling of the PBVMM filters [11–12].

The application of PBVMM has become popular in the field of structural dynamics due to its promise to extract subtle motion from video with a lower noise floor than other algorithms commonly employed for video motion measurement in structural dynamics, such as Digital Image Correlation (DIC) or edge detection [13–15]. PBVMM has been applied as a preprocessing step in the extraction of structural motion using another optical flow algorithm because of its ability to improve the noise floor of the measurement by amplifying motion that is

* Corresponding author at: University Ave, Lowell, MA 01854, USA.
E-mail address: zhu_mao@uml.edu (Z. Mao).

https://doi.org/10.1016/j.measurement.2021.109211
Received 4 November 2020; Received in revised form 26 January 2021; Accepted 21 February 2021
Available online 28 February 2021

below the noise floor of the final motion estimation algorithm [16]. This paper will give an explanation for why a noise floor improvement is achieved. Preprocessing video with PBVMM prior to DIC has been used on a several structures including wind turbine blades and rocket nozzels [16–18]. PBVMM has also been employed to study 3D motions using stereophotogrammetry [19–20]. In this case, PBVMM is applied to the output of the camera pair used for stereophotogrammetry prior to disparity calculations between each camera's images.

The noncontact study of internal volumetric motions has been widely used in the biomedical field with X-Ray Computed Tomography (CT) and Magnetic Resonance Imaging (MRI) to capture images of the heart and other organs deforming over time [21–22]. The adaption of these imaging techniques to other fields has led to the development of specialized algorithms for the extraction of motion from the volumetric images generated by these techniques. For use with CT, Digital Volume Correlation (DVC) an extension of DIC into 3D has been developed, and found widespread use in the study of material properties of composite structures [23–25]. DVC has been grown from developments in 2D DIC, with many of the improvements made in 2D algorithms, being generalized to the higher dimensional DVC case [44,45]. The special ability of MRI to tag volumes with spatially varying sinusoidal magnetic patterns has led to the development of the Harmonic Phase Algorithm (HARP) which tracks spatial motion of the induced patterns [26]. This technique is primarily used to study heart and brain motions [27–29]. Additionally, direct phase-based motion measurement has been develeoped for 2D external structural measurments, using sinusoidal patterning, in a process similar to HARP [30]. PBVMM has been applied to look at subtle motion of the brain during impacts, with 2D video slices taken from volumes captured using MRI and ultrasound [31–32]. The desire to capture high speed internal events has led to the development of Echo MRI which can capture an MRI volume in 50 ms, and has allowed for the study of rapid deformations of the brain using HARP [33–34]. Also, the technique of Multi-Sector CT has allowed for the study of periodic motions with effective sampling periods that have the potential to approach 1 ms for regularly repeating motion without significant phase noise [35].

The use of PBVMM to study internal slices from MRI and ultrasound images in [31,32] along with the continued application of volumetric imaging to medical images [33,34] shows a clear need for VMM in the field of internal motion anlaysis. Since PBVMM is a useful tool for enhancing motion extraction in these applciations, the ability to analyze the full volume with VMM will be benifitial to this type of research.

Part of the novel contribution of this work is the development of the 3D complex steerable pyramid, which is a 3D phase-based motion estimation technique. Prior work on 3D phase-based motion estiamtion has focused primarily on the use of Gabor transforms for motion estimation [46,47,48]. No attempts have been made to use a 3D complex steerable pyramid for volumetric motion estimation, as in this work. The 2D complex steerable pyramid and other localized phase extraction filters have been used in multiple sources for motion estiamtion in video [49–51].

In mechanical engineering, internal motion measurement using x-ray imaging and DVC is a growing field particularly for material science. Material characterization and compononent deformation has been measured with DVC in order to obtain full volume material dynamic behavior [40–41]. Additionally, the technique of X-Ray stereo imaging has been explored to capture internal 3D images of a structure and the associated dynamics of internal components [42].

VMM has the potential to build alongside these volumetric imaging and analysis tools to improve the extraction of subtle internal motion leveraging the volume image acquisition tools and the volumetric motion measurement tools that have been developed in the past. The technique presented in this paper is a novel method for analyzing 3D motion. The new approach represents an original extension of Phase-based Motion Magnification, which improves upon the state of the art in digital volumetric motion measurement with an order of magnitude lower motion noise than DVC. The effectiveness of VMM is compared to DVC and demonstrated both qualitatively and quantitatively on a representative volumetric structures.

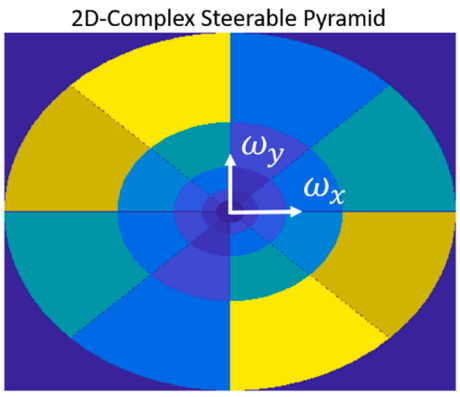

Fig. 1. The idealized filters of the complex steerable pyramid. The filters shown here are constructed with octave bandwidth in the radial frequency direction and 4 orientations.

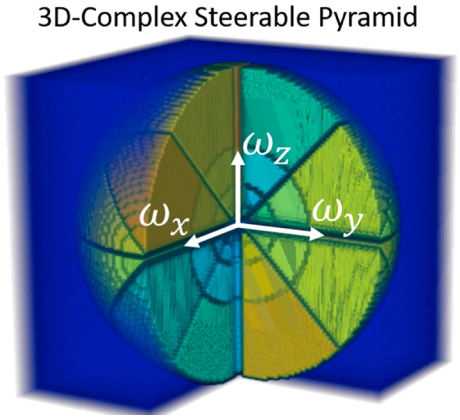

Fig. 2. The idealization of a complex steerable pyramid in 3 dimensions. The filters shown here are constructed with 4 orientations in each direction of rotations and octave bandwidth in the radial frequency direction. Low pass residual at the origin and high pass residual surrounding the shell of bandpass filters (dark blue).

Following this introduction, the paper is organized with a background, presenting relavent theory and the authors' contribution to the theory. Then a qualitative demonstration of the proposed technique for the visualization of subtle volumetric motion is presented. Next a quantitative demonstration of the VMM algorithm for the measurement of subtle motion when paired with DVC is shown. Finally, conclusions and future work are provided.

2. Background

2.1. Three-dimensional complex steerable pyramid

VMM makes use of a three-dimensional steerable pyramid based on the 2D steerable pyramid presented by Simoncelli et al. [36]. The 2D steerable pyramid creates a filter bank of localized orthogonal complex-valued filters by subdividing the Fourier spectrum in bands of orientation and frequency. Fig. 1, shows the idealized steerable pyramid for octave subdivisions in frequency and 4 orientations of filters.

The steerable pyramid in Fig. 1 can be extended to 3D space, using the same rules as for the 2D case. The filters remain related by rotations, dilations, and translations, with the 3D cases using an additional rotation direction to describe the filters. Fig. 2 shows a cutaway of the 3D

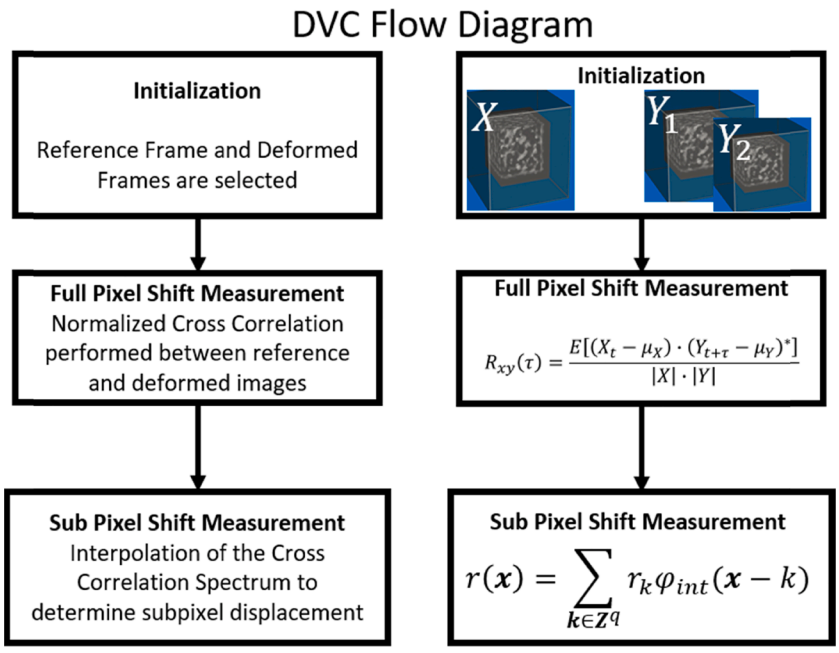

Fig. 3. DVC subpixel motion measurement process. On the right, X(t) is the reference image, Y(τ) is the translated image at time t+τ, R is the cross power spectrum, r is the normalized cross correlation, φ_{int} is an interpolation kernel, k is the number of discrete sample points in the image dimension q.

Fourier domain overlaid with the idealized filters of the 3D complex steerable pyramid.

The filters used to create the 3D complex steerable pyramid in this work follow the same criteria set in [35].

i) Band limiting (to prevent aliasing in the sub sampling operation):

$$L_1(\omega) = 0 for |\omega| > \frac{\pi}{2}$$

ii) Flat System Response:

$$|H_0(\omega)|^2 + |L_0(\omega)|^2 \left[|L_1(\omega)|^2 + |B(\omega)|^2 \right] = 1$$

iii) Recursion:

$$|L_1(\omega/2)|^2 = |L_1(\omega/2)|^2 \left[|L_1(\omega)|^2 + |B(\omega)|^2 \right]$$

where $H_0$and $L_0$are high and low pass filters which pre-process the system, L_1 is a recursively down sampled low pass filter, and B is a radial mask function.

These rules serve as the template for defining the octave bandwidth complex steerable pyramid. By selecting a 3D filter set that satisfies these properties, the 3D complex steerable pyramid can be created with the same properties as the steerable pyramid of Simoncelli and Freedman. This filter bank is used in the VMM process to extract local phase information from volumes.

To approximate the 3D filters which follow these rules, we use a raised cosine similar to that employed in [1] to better approximate a Gaussian curve.

2.2. Phase-based motion magnification

This work is a dimensional extension of PBVMM and as such the notation in deriving the theory will be consistent with those in [1].

Phase-Based Motion Magnification uses the response of the complex steerable pyramid to extract motion information based on the Fourier Shift Theorem, the principle that displacement of a signal is proportional to the phase output of the Fourier filter. Wadhwa et al. [1] demonstrates this principle in Equation (1) for the case of a Gaussian envelope with standard deviationσ, showing that the envelope shape does not affect the phase of the impulse response $S_\omega(x, t)$of the filter, and as such the calculation of phase under the filter is proportional to motion$\delta(t)$.

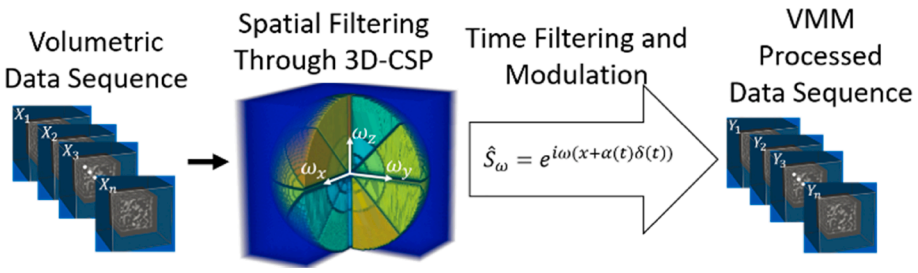

Fig. 4. Work flow diagram of volumetric motion magnification. First, a sequence of sequentially deforming volumetric images is collected. Second, each image is filtered by the complex steerable pyramid. Third, the phase of the complex response from the CSP is filtered. Finally, the modified phase information is used in the inverse CSP to construct a new volumetric image sequence with modified motion.

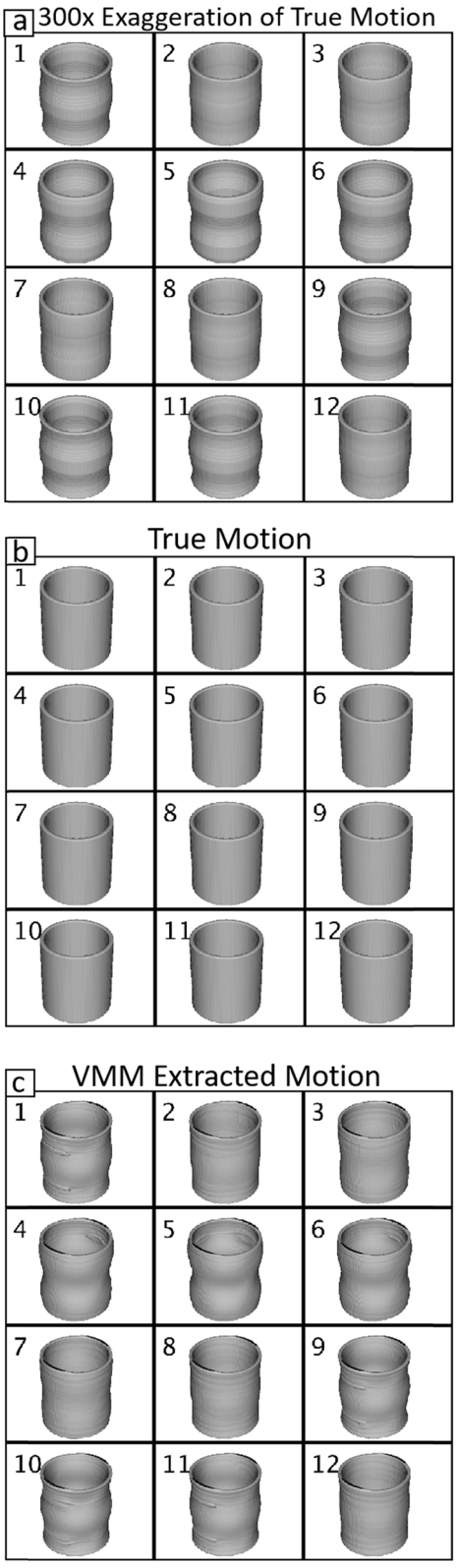

Fig. 5. The visualization of otherwise invisible subtle motion using VMM. The data set shown is the artificial modal motion of a cylinder with surface deformation given by equation (16). a) The exaggeration of the subtle motion of the test data, A = 3pixels. b) The true motion of the test data, A = $\frac{1}{100}$pixels. c) The result of applying VMM to the subtly deforming data of (b). VMM Parameters: 300x phase amplification, complex steerable pyramid built with half-octave and 10 orientations in each direction.

Table 1
The motion applied to the internal cube.

Applied Motion	
X-Motion	$\frac{1}{2}\sin\frac{2\pi t}{64}+\frac{1}{1000}\sin\frac{2\pi t}{10}$
Y-Motion	$\frac{3}{4}\cos\frac{2\pi t}{64}+\frac{1}{1000}\cos\frac{2\pi t}{10}$
Z-Motion	$\sin\frac{2\pi t}{64}+\frac{1}{1000}\cos\frac{2\pi t}{10}$

Table 2
Description of the test conducted to demonstrate the ability of VMM to qualitatively extract subtle motion alongside DVC.

Case	Case Description	Figure
1	DVC is applied to the internally moving cube of Fig. 5 with motion defined by Table 1.	6
2	The results of DVC shown in Fig. 6 are band pass filtered around F = 0.2π rad/sample.	7
3	VMM is applied to the data set with 1200x phase magnification, and band pass filter around F = 0.2π rad/sample. DVC is then applied to the VMM result. Finally, the DVC results are band pass filtered around F = 0.2π rad/sample.	8

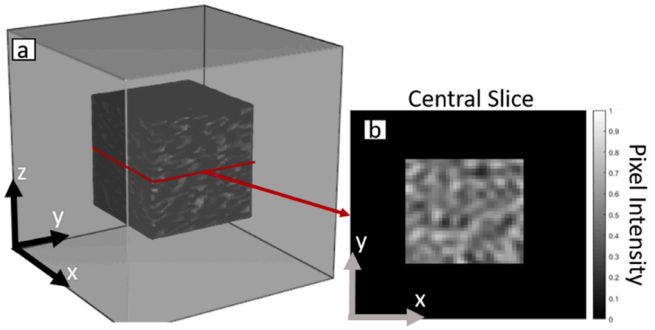

Fig. 6. The first frame of the generated data set used for a DVC test of VMM. a) One frame of the volumetric test data. A cube made of spatially-band-limited noise embedded in a larger volume of visually opaque material. b) The cross section of the volume through the central x-y slice.

$$S_\omega(x,t) = e^{-(x-\delta(t))^2/(2\sigma^2)}e^{2\pi i(x-\delta(t))} \tag{1}$$

The phase can then be processed over time by filtering or modulation, to separate, amplify, and attenuate motion present within an image sequence. This process produces a new imaginary filter response $\widehat{S}$with displacement modulated by $(1+\alpha)$:

$$\widehat{S}_\omega = e^{i\omega(x+(1+\alpha)\delta(t))} \tag{2}$$

where (1 + α) is the magnification coefficient.

In reality, the filters used for motion magnification from the complex steerable pyramid are defined with a flat system response, not a Gaussian. If the filters used in the complex steerable pyramid do not have a linear phase impulse response, the resulting frequency dependent phase delay of the filter will result in phase response of the filter not being perfectly proportional to the true motion. This means that if the filter is not linear-phase, the motion isn't guaranteed to be linearly separable from the filter response by its phase magnitude.

The 3D complex steerable pyramid is applied as a simple convolution between a volumetric image and the bank of pyramid filters described above. The response of each filter is stored as the localized, oriented, complex response to the spatial filter applied. The differences in these filter responses between sequentially deformed images, reveals motion in proportion to phase change.

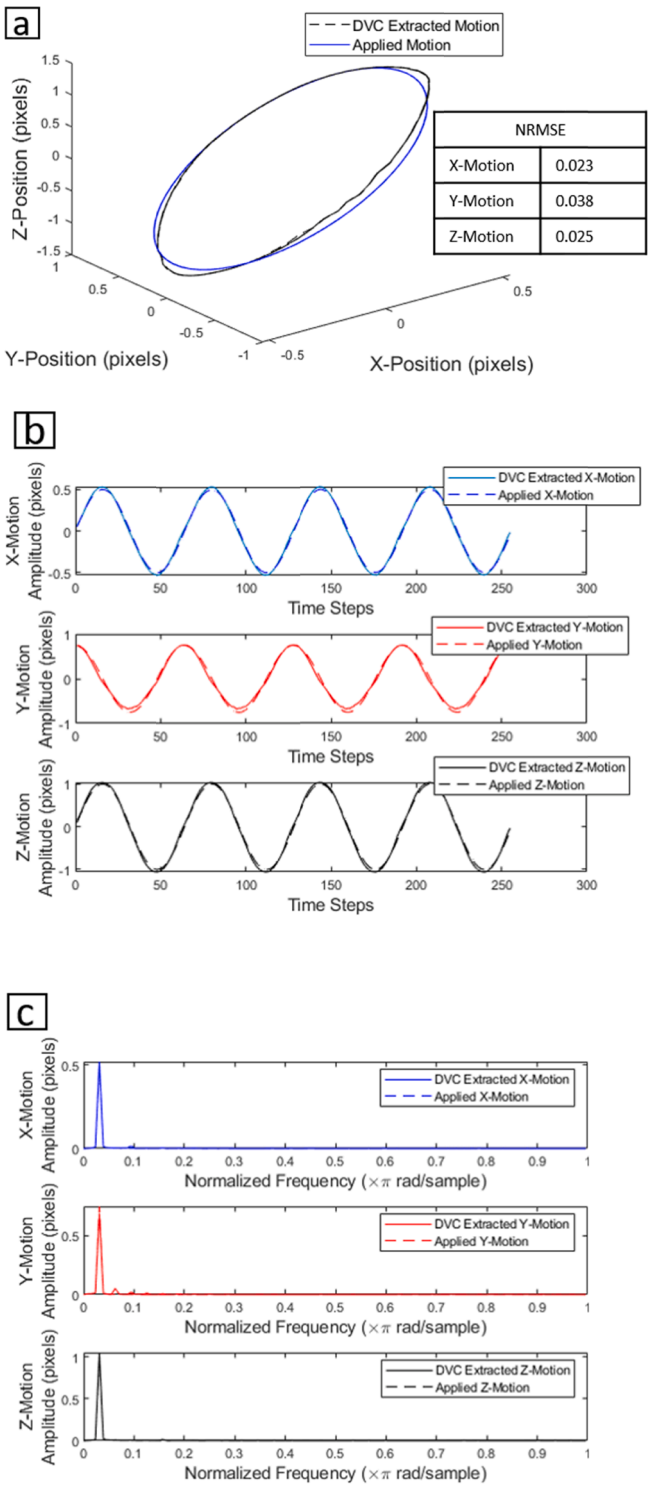

Fig. 7. Case 1: DVC is applied to the internally moving cube of Fig. 5 with motion defined by Table 1. The NRMSE for the x-y-z motion is also shown. (a) The orbit of the cube measured with DVC against the applied motion. (b) The time series of the x-y-z motion measured with DVC compared against the applied motion. (c) The x-y-z motion measured with DVC in the frequency domain.

This section presents the basic processes of phase-based motion magnification. It describes how the phases derived from the complex steerable pyramid filtering of an image are modified to generate motion magnified images.

2.3. Digital volume correlation

A focus of this work is the use of VMM as a pre-processing step for volumetric digital motion measurement algorithms. Digital volume correlation (DVC) is a robust and well-validated volumetric motion measurement tool popular for the study of deformable bodies. DVC uses subpixel interpolation of a normalized 3D cross-correlation to derive relative motion between volumes over time. The DVC algorithm is outlined in Fig. 3.

Many other interpolation schemes can be used to estimate the subpixel displacement at a location including iterative approaches and linear kernel based interpolation [37].

3. Discussion

In this section, Video Motion Magnification is demonstrated on synthetic 4D data. Two separate tests are conducted to illustrate the effectiveness of the technique and the feasibility applied to enhance VMM. First, a qualitative example is shown on how VMM can be applied to visualize the subtle deformation of a 3D cylinder animated with subpixel modal deformations. Second, VMM is demonstrated as a tool for preprocessing a volume sequence prior to performing DVC in order to extract motion otherwise below the DVC noise floor.

VMM is applied to a sequence of images following the work flow of Fig. 4.

3.1. Qualitative visualization of subtle modal motion

A cylinder was generated in slices by rotation of a line about an endpoint to create a stack of circles. Over time steps$t$, the radius of each slice's circle was altered by interpolation based on vertical position z within the data set and time, so that the change in radius Δr of the cylinder was defined over time by

$$\Delta r(z,t) = A\cos\left(\frac{2\pi t}{10}\right)\sin\left(\frac{2\pi z}{L}\right) \tag{16}$$

where A is the maximum amplitude of the induced motion, L is the length of the cylinder, and $t = 1, 2, 3\cdots$

A test structure was created using the defined normal modal motion of Equation (16) with $A = 0.01$*pixels* over 12-time steps. VMM was then applied to this data-set and the phase was amplified 300 times to produce a new 4D data set with easily visualizable motion. Fig. 4 shows montages of: (a) the 300x exaggerated motion of the volume (what the data is really doing but exaggerated 300x for visualization), (b) The true motion over time with $A = 0.01$pixel, (c) The results of applying 300x VMM to the subtle motion data.

Qualitatively, the VMM results contain the spatially smoothed deformations that were applied in the artificial data set. The use of VMM in this case allows for the visual identification of subtle motions that are otherwise invisible in the raw data. Visible within Fig. 4c) are artifacts located at regions of largest displacement, resulting from filter ringing and spectral truncation as in PBVMM.

3.2. Quantitative enhancement of the DVC noise floor using VMM

A second test was conducted to demonstrate how VMM can be applied to a 4D data set in order to filter and increase the magnitude of subtle motion in the data, so it can be measured with DVC. DVC in this test is performed using the freely available and state-of-the-art algorithm of [37]. By using this algorithm for comparison with VMM, it can be seen how well VMM performs relative to the current state of the art in DVC.

To emulate a tumor moving within a body, a cube of band-limited noise was embedded within a larger cube of constant intensity. A single volumetric frame of this data is shown in Fig. 5 along with a cross section of the volume.

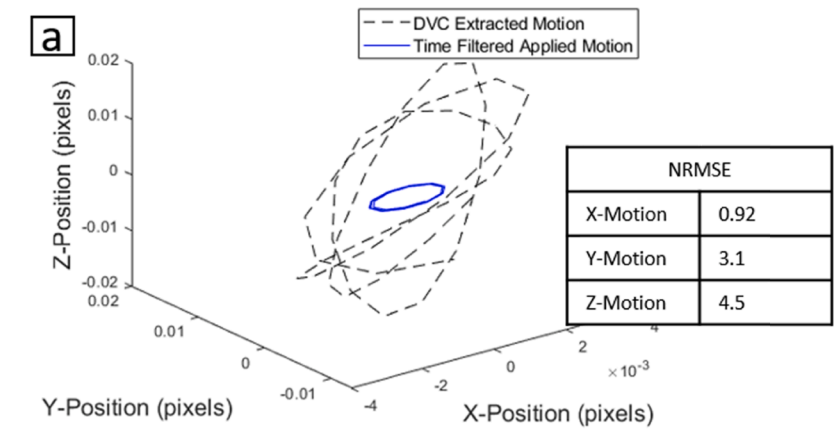

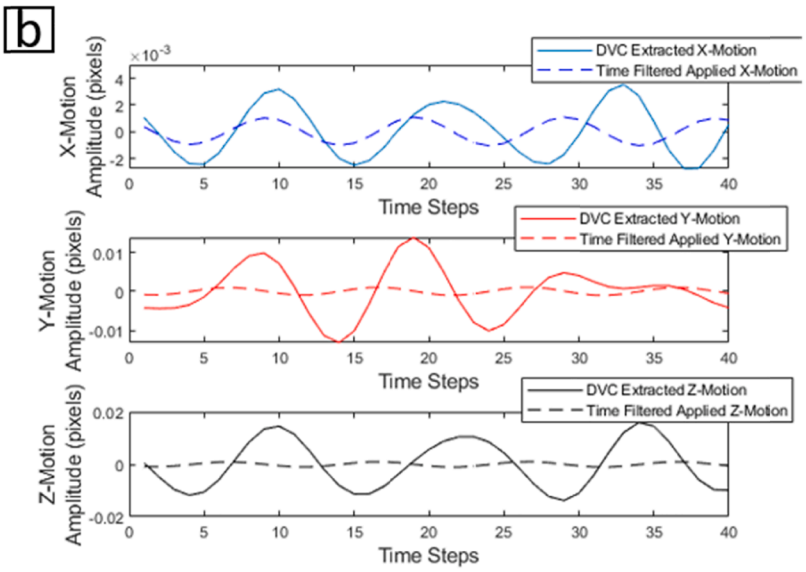

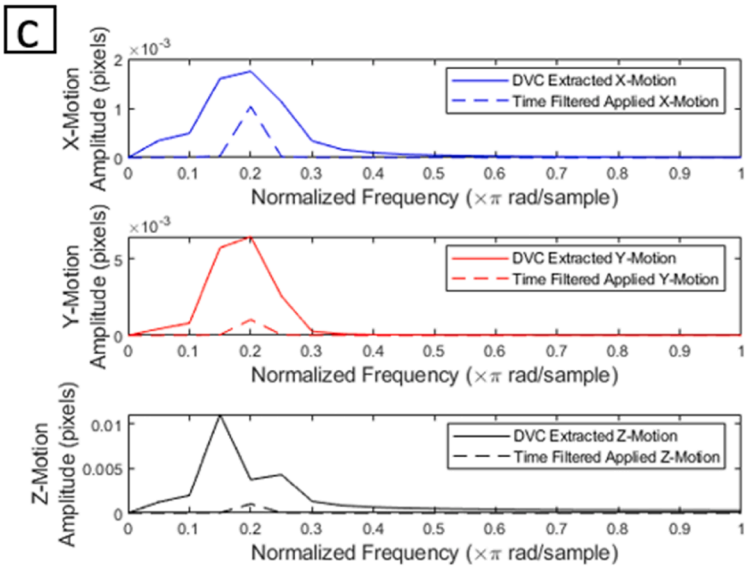

Fig. 8. Case 2: *The results of DVC shown in Fig. 6 are band pass filtered around $F = 0.2\pi$ rad/sample. The goal of this is to extract the subtle motion at this frequency from the DVC results. (a) The orbit of the cube measured by filtering the DVC results against the filtered applied motion. (b) The time series of the x-y-z motion measured by filtering the DVC results, compared against the filtered applied motion. (c) The comparison of (b) in the frequency domain. The results show that the subtle high frequency content of the motion was not captured by DVC. Instead, because the motion was below the DVC noise floor, only band limited noise is obtained in the process.*

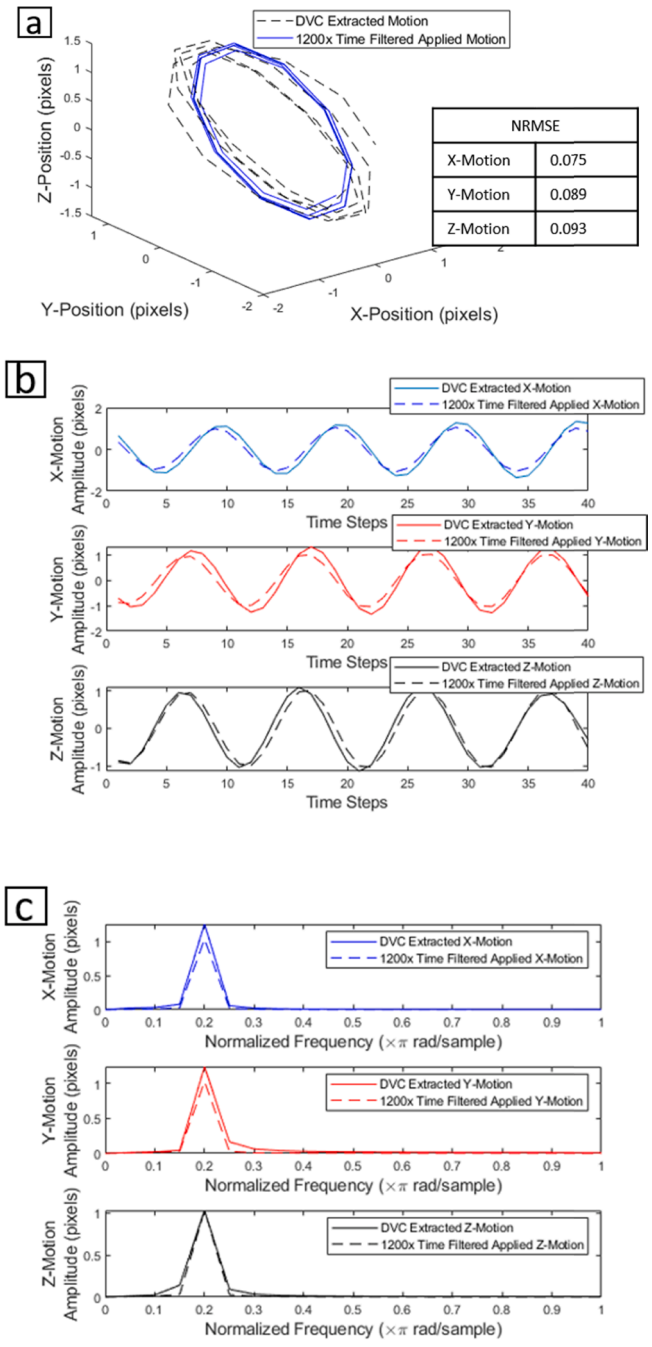

Fig. 9. Case 3: VMM is applied to the data set with 1200x phase magnification, and band pass filter around F = .2πrad/sample. DVC is then applied to the VMM result. Finally, the DVC results are band pass filtered around F = .2πrad/sample. The motivation is to use VMM to improve the motion amplitude and SNR of DVC so the subtle motion can be measured. (a) The orbit of the cube measured using VMM and DVC, compared against the exaggerated filtered applied motion. (b) The time series of the x-y-z motion measured using VMM and DVC, compared against the exaggerated filtered applied motion. (c) The comparison of (b) in the frequency domain. This example shows how VMM can be used to preprocess a 4D data set prior to DVC in order to filter and extract subtle motion that is otherwise buried within the DVC noise floor.

The internal cube was then translated over time using spatial linear interpolation in 3 dimensions with the motion described in Table 1 to produce 256 frames of 3D data with internal deformation. Finally, 1% uniformly distributed spatial noise was added to the 4D data to simulate measurement error. This noise level is selected to be representative of extreme noise levels seen in MRI volumes [31,52].

The data set described was analyzed with DVC and VMM in the 3 test cases described in Table 2. The goal of these tests is to extract the subtle x-y-z motion at F = 0.2π rad/sample, applied to the internal cube by Table 1.

The results are compared statistically based on the amplitude normalized root mean square error (NRMSE), defined here. The NRMSE is displayed on plot (a) of each of the following Figs. 6-8 to give a comparable measure of accuracy, between the test cases. Fig. 9.

$$NRMSE = \frac{\sqrt{\sum \left[x_{applied} - x_{measured}\right]^2}}{\left|\max\left(x_{applied}\right) - \min\left(x_{applied}\right)\right|} \tag{17}$$

The DVC Results of test case 1 were then band pass filtered around F = 0.2π rad/sample in an attempt to extract the subtle high frequency component of the applied motion, using a 3-pole Butterworth filter with poles at $0.15\pi and 0.25\pi rad/sample$. The last 40 points of the data are shown in Fig. 6, leaving out the transients induced by the filter on the short time series.

Fig. 7 shows that the noise floor of the DVC for this data is in the region of a 10th of a pixel, an order of magnitude above motion at the normalized frequency of 0.2π radians/sample. This noise floor makes it impossible for DVC to capture the subtle motion of interest by itself.

The next step (Case 3) was to apply VMM to the data set prior to performing DVC. The data set was decomposed into the 3D complex steerable pyramid, and the resulting phases were filtered using the same 3-pole Butterworth filter with poles at $0.15\pi and 0.25\pi rad/sample$, then magnified by a factor of 1200. The pyramid was inverted and the result was analyzed with DVC. Finally, the DVC result was filtered again by the same 3-pole Butterworth filter described. The results of this procedure are shown in Fig. 8. Again, the last 40 data points are shown, leaving out the preceding data heavily corrupted by filter transients.

The results of Fig. 8 show a significant improvement in the ability to extract the subtle motion of interest from the 4D data of the internally moving cube. Overall, an order of magnitude improvement in noise floor is achieved between test Case 2 and test Case 3. This shows that VMM is an effective tool for the extraction and quantification of subtle volumetric motion. Using the presented technique, we were able to reduce the NRMSE of the subtle motion extracted with DVC from over 300% to less than 10%. This result represents an order of magnitude improvement in error, and demonstrates how VMM is able to lower the noise floor of digital volumetric motion measurement from DVC's current state of the art. This is a considerable improvement that has the potential to open up previously under studied levels of internal motion and has the potential to be applied to a wide range of applications (e.g. biomedical imaging and dynamic material characterization).

4. Conclusion

This work develops Volumetric Motion Magnification, a novel extension of Phase-based Motion Magnification into three-dimensions. The effectiveness of Volumetric Motion Magnification is demonstrated both qualitatively and quantitatively for the extraction of subtle internal localized volumetric motion. The technique is demonstrated to be capable of extracting motion alongside Digital Volume Correlation with a noise floor an order of magnitude better than with Digital Volume Correlation alone.

The main limitations of VMM are first, acquiring 4D data is expensive, time consuming, and produces data with poor time resolution. VMM is also limited in the same ways as PBVMM, computation times can be excessive (running into multiple days on a desktop computer), with large data sets of many gigabytes and similarly sized filter banks. Also, VMM suffers from generation of artifacts and degradation of reconstructed images due to the filtering process. Despite of the aforementioned limitations of VMM, the proposed approach has shown to be an effective algorithm to greatly enhance the state of the art in subtle volumetric motion extraction.

In the future, analysis of real volumetric images is a desired extension of this work, yet the biggest challenge for the application of the VMM algorithm to real data is the determination of appropriate time filters and modulation factors for the data set being examined. In the demonstration shown in this paper where motion properties are known, the selection of filters and amplification is relatively less challenging. For the case of the real 4D data set, the problem is more complicated. One possible solution is the use of additional contact sensors for the capture of motion frequency. For instance, an accelerometer placed on the casing of a structure of interest could reveal a power spectrum of vibration, which may be leveraged as a starting point for filter design. At this time, VMM will require an iterative approach to the estimation of amplification and filter parameters for the effective analysis of real world data.

Overall, this work develops a powerful new tool for the study of internal motion. The advent of VMM will allow the study of subtle motions that are impossible to detect or measure with the state of the art. VMM is a novel development that has the potential to open new avenues of internal dynamics material research.

Declaration of Competing Interest

The authors declared that there is no conflict of interest.

Acknowledgements

This work is supported by the National Science Foundation under Grant No. 1762809. Any opinions, findings, and conclusions or recommendations expressed in this material are those of the authors and do not necessarily reflect the views of the National Science Foundation. The authors would also like to acknowledge the discussion with Sandia National Laboratories and their support through Purchase Order #2172799.

References

[1] N. Wadhwa, M. Rubinstein, F. Durand, W.T. Freeman, Phase-based video motion processing, ACM Trans. Graphics (TOG) 32 (4) (2013) 80.
[2] Tianfan Xue, Michael Rubinstein, Neal Wadhwa, Anat Levin, Fredo Durand, and William T Freeman. Refraction wiggles for measuring fluid depth and velocity from video. In ECCV, 2014.
[3] J. G. Chen, N. Wadhwa, Y.-J. Cha, F. Durand, W. T. Freeman, and O. Buyukozturk. Structural modal identification through high speed camera video: Motion magnification. In Topics in Modal Analysis I, Volume 7, pages 191–197. Springer, 2014.
[4] A. Davis, M. Rubinstein, N. Wadhwa, G.J. Mysore, F. Durand, W.T. Freeman, The visual microphone: passive recovery of sound from video, ACM Trans. Graphics (TOG) (2014).
[5] A. Davis, Katherine L Bouman, Justin G Chen, Michael Rubinstein, Frédo Durand, and William T Freeman, Estimating material properties from small motions in video. In CVPR, Visual Vibrometry, 2015.
[6] Y. Zhang, S.L. Pintea, and J, C. van Gemert. Video acceleration magnification, In Computer Vision and Pattern Recognition, 2017.
[7] X. Wu, X. Yang, J. Jin, Z. Yang, Amplitude-Based Filtering for Video Magnification in Presence of Large Motion, Sensors. 18 (2018) 2312, https://doi.org/10.3390/s18072312.
[8] M.A. Elgharib, M. Hefeeda, F. Durand, W.T. Freeman, Video magnification in presence of large motions, CVPR 2015 (2015) 4119–4127.
[9] N. Wadhwa, M. Rubinstein, F. Durand, W.T. Freeman, Riesz pyramid for fast phase-based video magnification, Computational Photography (ICCP), 2014 IEEE International Conference on, IEEE (2014).
[10] Wadhwa, N., Rubinstein, M., Durand, F., Freeman, W.T.: Quaternionic Representation of the Riesz Pyramid for Video Magnification, http://people.csail.mit.edu/nwadhwa/rieszpyramid.
[11] T.-H. Oh, R. Jaroensri, C. Kim, M. Elgharib, F. Durand, W.T. Freeman, W. Matusik, Learning-based video motion magnification, Proceedings of the European Conference on Computer Vision (ECCV) (2018) 633–648.
[12] J.F. Kooij, J.C. van Gemert, Depth-aware motion magnification, ECCV (2016).
[13] A. Sarrafi, Z. Mao, C. Niezrecki, P. Poozesh, Vibration-based damage detection in wind turbine blades using phase-based motion estimation and motion magnification, J. Sound Vib. 421 (2018) 300–318.
[14] M. Civera, L. Zanotti Fragonara, C. Surace, An experimental study of the feasibility of phase-based video magnification for damage detection and localisation in operational deflection shapes, Strain 56 (2020) e12336.
[15] Y. Yang, C. Dorn, T. Mancini, Z. Talken, G. Kenyon, C. Farrar, D. Mascarenas, Blind identification of full-field vibration modes from video measurements with phase-based video motion magnification, Mech. Syst. Sig. Process. 85 (2017) 567–590, https://doi.org/10.1016/j.ymssp.2016.08.041.
[16] M.A. Eitner, B.G. Miller, J. Sirohi, C.E. Tinney, Operational modal analysis of a thin-walled rocket nozzle using phase-based image processing and complexity pursuit, in: C. Niezrecki, J. Baqersad, D. Di Maio (Eds.), Rotating machinery, optical methods & scanning LDV methods, Springer International Publishing, 2019, pp. 19–29.
[17] Á.J. Molina-Viedma, E. López-Alba, L. Felipe-Sesé, F.A. Díaz, Operational Deflection Shape Extraction from Broadband Events of an Aircraft Component Using 3D-DIC in Magnified Images, Shock Vib. 2019 (2019) 1–9, https://doi.org/10.1155/2019/4039862.
[18] V. Fioriti, I. Roselli, A. Tati, R. Romano, G. De Canio, Motion Magnification Analysis for structural monitoring of ancient constructions, Measurement 129 (2018) 375–380.
[19] P. Poozesh, A. Sarrafi, Z. Mao, P. Avitabile, C. Niezrecki, Feasibility of extracting operating shapes using phase-based motion magnification technique and stereo-photogrammetry, J. Sound Vib. 407 (2017) 350–366.
[20] A. Molina-Viedma, L. Felipe-Sesé, E. López-Alba, F. Díaz, 3D mode shapes characterisation using phase-based motion magnification in large structures using stereoscopic DIC, Mech. Syst. Signal Process. 108 (2018) 140–155.
[21] W.R. Hendee, E.R. Ritenour, Medical Imaging Physics, 4 ed., John Wiley & Sons, New York, NY, USA, 2002.
[22] B. Desjardins, E.A. Kazerooni, ECG-gated cardiac CT, AJR 182 (2004) 993–1010.
[23] B.K. Bay, et al., Digital volume correlation: Three-dimensional strain mapping using X-ray tomography, Exp. Mech. 39 (3) (1999) 217–226.
[24] V. Cnudde, M.N. Boone, High-resolution X-ray computed tomography in geosciences: a review of the current technology and applications, Earth-Sci. Rev. (2013).
[25] R. Waymel, E. Quintana, S. Kramer, K. Long, D. Bolintineanu, Using X-ray Micro-Computed Tomography and –Digital Volume Correlation to Investigate the Microstructure of Elastomeric Foams, Sandia Natl. Labs. (2018).
[26] L. Axel, L. Dougherty, MR Imaging of Motion with Spatial Modulation of Magnetization, Radiology 171 (1989) 841–845.
[27] J.L. Prince, E.R. McVeigh, Motion estimation form tagged MR image sequences, IEEE Trans. Med. Imag. 11 (1992) 238–249.
[28] N.F. Osman, E.R. McVeigh, J.L. Prince, Imaging heart motion using harmonic phase MRI IEEE Trans, Imaging at press, Med, 2000.
[29] P.V. Bayly, S. Ji, S.K. Song, R.J. Okamoto, P. Massouros, G.M. Genin, Measurement of strain in physical models of brain injury: a method based on HARP analysis of tagged magnetic resonance images (MRI), J. Biomech. Eng. 126 (2004) 1–6.
[30] M. Southwick, Z. Mao, and C. Niezrecki. "A Complex Convolution Kernel-Based Optical Displacement Sensor." IEEE Sensors. VOL. 20, NO. 17, SEPTEMBER 1, 2020.
[31] I. Terem, W.W. Ni, M. Goubran, M.S. Rahimi, G. Zaharchuk, K.W. Yeom, M. E. Moseley, M. Kurt, S.J. Holdsworth, Revealing sub-voxel motions of brain tissue using phase-based amplified MRI (aMRI), Magn. Reson. Med. 80 (2018) 2549.
[32] V. Perrot, S. Salles, D. Vray, H. Liebgott, Video Magnification Applied in Ultrasound, IEEE Trans. Biomed. Eng. 66 (1) (2019) 283–288, https://doi.org/10.1109/TBME.2018.2820384.
[33] M.K. Stehling, R. Turner, P. Mansfield, Echoplanar imaging: Magnetic resonance imaging in a fraction of a second, Science 254 (1991) 43–50.
[34] M. Poustchi-Amin, S.A. Mirowitz, J.J. Brown, R.C. McKinstry, T. Li, Principles and applications of echo-planar imaging: a review for the general radiologist, Radiographics 21 (2001) 767–779.
[35] Yin et al. Multi-Sector Computed Tomography Image Acquisition. U.S. Patent 9,042,512. issued May 26, 2015.
[36] E. P. Simoncelli and W T Freeman. The Steerable Pyramid: A Flexible Architecture for MultiScale Derivative Computation. IEEE Second Int'l Conf on Image Processing. Washington DC, October 1995.
[37] J. Yang, L. Hazlett, A. Landauer, C. Franck, Augmented Lagrangian Digital Volume Correlation, Exp. Mech. (2020).
[40] E.; Reu, P.;Wag, E. Jimenez, K. Thompson, S. Kramer. "Digital Volume Correlation for Materials Characterization." 19th World Conference on Non-Destrcutve Testing. 2016.
[41] D.P. Finegan, E. Tudisco, M. Scheel, J.B. Robinson, O.O. Taiwo, D.S. Eastwood, P. D. Lee, M. Di Michiel, B. Bay, S.A. Hall, G. Hinds, D.J.L. Brett, P.R. Shearing, Quantifying Bulk Electrode Strain and Material Displacement within Lithium Batteries via High-Speed Operando Tomography and Digital Volume Correlation, Adv. Sci. 3 (2015) 1500332.
[42] E. Jones, E. Quintana, P. Reu, J. Wagner, X-Ray stereo digital image correlation, Exp. Tech. 44 (2019) 159–174.
[44] A. Kojima, N. Sakurai, and J. Kishigami, "Motion Detection Using 3D-FFT Spectrum," Proc. of IEEE ICASSP' 93, Minneapolis, Minnesota, April 27-30, pp. 213-216.
[45] Buljac, A.; Jailin, C.; Mendoza, A.; Neggers, J.; Taillandier-Thomas, T.; Bouterf, A.; Smaniotto, B.; Hild, F.
[46] S. Roux, Digital volume correlation: Review of progress and challenges, Exp. Mech. 58 (2018) 661–708.
[47] T.R. Reed, On the Computation of Optical Flow using the 3-D Gabor Transform, Multidimension. Syst. Signal Process. 9 (1998) 447–452.
[48] Z. Qian, D. N. Metaxas and L. Axel, "Extraction and Tracking of MRI Tagging Sheets Using a 3D Gabor Filter Bank," 2006 International Conference of the IEEE Engineering in Medicine and Biology Society, New York, NY, 2006, pp. 711-714, doi: 10.1109/IEMBS.2006.259542.

[49] T. Chen, X. Wang, S. Chung, D. Metaxas, L. Axel, Automated 3D Motion Tracking Using Gabor Filter Bank, Robust Point Matching, and Deformable Models, IEEE Trans. Med. Imaging 29 (1) (2010) 1–11, https://doi.org/10.1109/TMI.2009.2021041.

[50] Samson Timoner, Dennis Freeman, Multi-image gradient-based algorithms for motion estimation, Optical Engineering – Opt. Eng. 40 (2001), https://doi.org/10.1117/1.1391495.

[51] D.J. Fleet, A.D. Jepson, Computation of component image velocity from local phase information, Int. J. Comput. Vision 5 (1990) 77–104, https://doi.org/10.1007/BF00056772.

[52] E.R. McVeigh, R.M. Henkelman, M.J. Bronskill, Noise and filtration in magnetic resonance imaging, Med. Phys. 12 (5) (1985) 586–591, https://doi.org/10.1118/1.595679.